







ORIGINAL RESEARCH

# Hydrogen Sulfide Attenuates Lymphedema Via the Induction of Lymphangiogenesis Through a PI3K/Akt-Dependent Mechanism

Junya Suzuki , MD; Yuuki Shimizu , MD, PhD; Takumi Hayashi, MD; Yiyang Che, MD; Zhongyue Pu , MD, PhD; Kazuhito Tsuzuki, MD, PhD; Shingo Narita , MD; Rei Shibata, MD, PhD; Isao Ishii, PhD; John W. Calvert , PhD; Toyooki Murohara , MD, PhD

**BACKGROUND:** Accumulating evidence suggests that hydrogen sulfide ( $H_2S$ ), an endogenously produced gaseous molecule, plays a critical role in the regulation of cardiovascular homeostasis. However, little is known about its role in lymphangiogenesis. Thus, the current study aimed to investigate the involvement of  $H_2S$  in lymphatic vessel growth and lymphedema resolution using a murine model and assess the underlying mechanisms.

**METHODS AND RESULTS:** A murine model of tail lymphedema was created both in wild-type mice and cystathionine  $\gamma$ -lyase-knockout mice, to evaluate lymphedema up to 28 days after lymphatic ablation. Cystathionine  $\gamma$ -lyase-knockout mice had greater tail diameters than wild-type mice, and this phenomenon was associated with the inhibition of reparative lymphangiogenesis at the site of lymphatic ablation. In contrast, the administration of an  $H_2S$  donor, diallyl trisulfide, ameliorated lymphedema by inducing the formation of a considerable number of lymphatic vessels at the injured sites in the tails. In vitro experiments using human lymphatic endothelial cells revealed that diallyl trisulfide promoted their proliferation and differentiation into tube-like structures by enhancing Akt (protein kinase B) phosphorylation in a concentration-dependent manner. The blockade of Akt activation negated the diallyl trisulfide-induced prolymphangiogenic responses in lymphatic endothelial cells. Furthermore, the effects of diallyl trisulfide treatment on lymphangiogenesis in the tail lymphedema model were also negated by the inhibition of phosphoinositide 3'-kinase (PI3K)/Akt signaling.

**CONCLUSIONS:**  $H_2S$  promotes reparative lymphatic vessel growth and ameliorates secondary lymphedema, at least in part, through the activation of the Akt pathway in lymphatic endothelial cells. As such,  $H_2S$  donors could be used as therapeutics against refractory secondary lymphedema.

**Key Words:** Akt ■ diallyl trisulfide ■ hydrogen sulfide ■ lymphangiogenesis ■ lymphedema

Secondary lymphedema, resulting from lymphatic dysfunction caused by inadequate lymphatic drainage, occurs after lymph node dissection during surgery or radiation therapy of cancers such as breast and pelvic cancers.<sup>1,2</sup> This lymphedema is clinically challenging not only in terms of appearance but also in terms of poor quality of life because of limb dysfunction, development of skin ulcers, recurring pain, and infection (cellulitis). In the future, secondary lymphedema is expected

to become more prevalent among patients with cancer because of the extensive use of radical surgery and increased life expectancy of cancer survivors.<sup>1,2</sup> Current therapies are mainly focused on physical/symptomatic treatments, such as lymphatic drainage massage, wearing elastic stockings, and skin care; however, a fundamental treatment with a highly recommended class is still lacking.<sup>1</sup> Therefore, the development of a new therapy for refractory lymphedema is warranted. Therapeutic

Correspondence to: Yuuki Shimizu, MD, PhD, FESC, Department of Cardiology, Nagoya University Graduate School of Medicine, 65 Tsurumai, Showa-ku, Nagoya 466-8550, Japan. Email: [shimi123@med.nagoya-u.ac.jp](mailto:shimi123@med.nagoya-u.ac.jp)

Supplemental Material is available at <https://www.ahajournals.org/doi/suppl/10.1161/JAHA.122.026889>

For Sources of Funding and Disclosures, see page 12.

© 2022 The Authors. Published on behalf of the American Heart Association, Inc., by Wiley. This is an open access article under the terms of the [Creative Commons Attribution-NonCommercial-NoDerivs](https://creativecommons.org/licenses/by-nc-nd/4.0/) License, which permits use and distribution in any medium, provided the original work is properly cited, the use is non-commercial and no modifications or adaptations are made.

JAHA is available at: [www.ahajournals.org/journal/jaha](http://www.ahajournals.org/journal/jaha)

## CLINICAL PERSPECTIVE

### What Is New?

- Validation with genetically cystathionine  $\gamma$ -lyase-deficient mice showed that low hydrogen sulfide ( $H_2S$ ) levels cause reduced lymphangiogenesis and exacerbation of lymphedema in a mouse model of lymphedema.
- Administration of the  $H_2S$  donor diallyl trisulfide was shown to increase  $H_2S$  concentrations and promote lymphatic endothelial cell proliferation, migration, and tube formation, leading to therapeutic lymphangiogenesis.
- The mechanism of  $H_2S$ -mediated lymphangiogenesis indicates involvement of (phosphoinositide 3'-kinase (P13K))/Akt (protein kinase B) signaling.

### What Are the Clinical Implications?

- $H_2S$  was suggested to be a molecular target in therapeutic lymphangiogenesis.
- Administration of diallyl trisulfide, an  $H_2S$  donor, could be a therapeutic strategy for secondary lymphedema with no fundamental treatment.

## Nonstandard Abbreviations and Acronyms

<b>CSE</b>	cystathionine $\gamma$ -lyase
<b>DATS</b>	diallyl trisulfide
<b>LEC</b>	lymphatic endothelial cell
<b>POD</b>	postoperative day

lymphangiogenesis is an emerging treatment strategy to reconstruct the fragmented lymphatic network and thereby reinstate lymphatic function.<sup>3</sup>

In recent years, hydrogen sulfide ( $H_2S$ ), which exists only in trace amounts within the body, has been shown to play an important role in both physiological and pathological events, in a manner similar to other gaseous molecules such as NO and CO.<sup>4</sup>  $H_2S$  is produced by 3 enzymes, cystathionine  $\gamma$ -lyase (CSE), cystathionine  $\beta$ -synthase, and 3-mercaptopyruvate sulfur transferase. The expression of cystathionine  $\beta$ -synthase is located in the brain, and expression of CSE is located in smooth muscle, including in the vascular system, portal vein, and ileum, and of 3-mercaptopyruvate sulfur transferase in neurons and vascular endothelium.<sup>5,6</sup> These enzymes help maintain the physiological levels of  $H_2S$  for organ homeostasis.<sup>7</sup> In addition, organic sulfides, such as diallyl trisulfide (DATS), which is present in high concentrations in garlic, interact readily with thiol groups or thiol-containing compounds (eg, glutathione) found in biological systems to exogenously generate free  $H_2S$ .<sup>8</sup> Growing studies on  $H_2S$  for combating

cardiovascular diseases have demonstrated its cardioprotective effects. For instance, the benefits of  $H_2S$  have been elucidated in models such as pressure-overload heart failure models,<sup>9</sup> myocardial ischemia-reperfusion injury models,<sup>10</sup> and endoplasmic reticulum stress-reducing effect in high-fat diet models,<sup>11,12</sup> suggesting it is a potential therapeutic target.  $H_2S$  has also been demonstrated to promote angiogenesis, thereby restoring blood flow in ischemic limbs.<sup>13,14</sup> Meanwhile, the effect of  $H_2S$  on lymphangiogenesis is still unclear.

Accordingly, this study aimed to investigate the effect of  $H_2S$  on lymphangiogenesis. Furthermore, we explored the possibility of therapeutic lymphangiogenesis in a mouse tail lymphedema model using DATS, an  $H_2S$  donor.

## METHODS

Materials and methods are available within the article or supplemental material. The data, analytic methods, and study materials used in this study are available from the corresponding author upon reasonable request.

## Animal Care

All procedures for animal care and study were approved by the Animal Ethics Review Board of Nagoya University School of Medicine. Our study conformed to the guidelines from the Directive 2010/63/EU of the European Parliament on the protection of animals used for scientific purposes or the National Institutes of Health *Guide for the Care and Use of Laboratory Animals*. C57BL/6J male mice were obtained from Charles River Laboratories Japan (Kanagawa, Japan) and used as wild-type (WT) mice. CSE-knockout (KO) mice, generated in a C57BL/6J background, were provided by Professor Isao Ishii.<sup>15</sup>  $H_2S$  is produced not by a single cell but by multiple cells in the body. Furthermore, because  $H_2S$  is a gas, it can easily pass between cells regardless of the origin. Therefore, we did not use the tissue-specific CSE-KO mice; we used the global CSE-KO mice in this study. We used only male rats in the present in vivo studies as described in the Council on Arteriosclerosis, Thrombosis, and Vascular Biology statement because sex difference is considered a biological variable.<sup>16</sup> Mice were randomly assigned to experimental groups. All mice were anesthetized with a combination of hydrochloric acid medetomidine (0.3 mg/kg), midazolam (4 mg/kg), and butorphanol tartrate (5 mg/kg) before the surgical procedure. Cervical dislocation under anesthesia was performed as a strategy for euthanasia.

## Mouse Tail Lymphedema Model

WT and CSE-KO male mice (8–10 weeks old) were subjected to ablation of the tail surface lymphatic network by means of surgery under anesthesia, as described

previously.<sup>17,18</sup> In brief, a 2-mm-wide circumferential annulus of the skin, 10mm distal to the tail base, except for a 2-mm-square dermal flap located at the ventral side, was excised from the tail using a cautery knife (CHANGE-A-TIP Deluxe Low-Temperature Cautery Kit).<sup>17,18</sup> The subcutaneous lymphatic vessels were disturbed by this operation. Our model damaged not only capillary levels of lymphatic vessels but also collecting vessels existing on both sides of the mouse tail. In some mice, DATS was intraperitoneally injected once a day up to postoperative day (POD) 10, as described below. The extension of lymphedema was evaluated as tail diameter at a site 1 cm distal from the lymphatic segmentation site, as previously described.<sup>17</sup>

### Immunohistochemistry

Frozen sections were prepared from the tail at 28 days after the ablation surgery. The 8- $\mu$ m-thick sections were fixed in 4% paraformaldehyde, washed twice with PBS, and blocked with 0.5% FBS albumin at room temperature for 1 hour. Sections were then incubated with primary antibodies, anti-LYVE-1 (lymphatic vessel endothelial hyaluronan receptor 1) (1:125; Acris) or phospho-Akt (or Protein kinase B) (Cell Signaling Technology, CST; number 4060, 1:400), and anti-mouse podoplanin (1:250; R&D Systems) antibodies, at 4 °C overnight, followed by incubation with secondary antibodies, Alexa-Fluor 488-conjugated anti-rabbit (1:1000; Thermo Fisher Scientific) and Alexa-Fluor 594-conjugated anti-goat (1:1000; Thermo Fisher Scientific) antibodies, respectively, at room temperature for 1 hour.<sup>19-21</sup> The capillary density of lymphatic vessels was evaluated as LYVE-1 and podoplanin double-positive cells per field by previously established methods.<sup>17,19,21</sup> The nuclei were stained using 4',6-diamidino-2-phenylindole (1:1000; Dojindo), and macrophages were detected by phycoerythrin-labeled anti-mouse F4/80 monoclonal antibody (1:1000; BioLegend). Images were visualized using a BZ-X710 fluorescent microscope (KEYENCE), with a  $\times$ 20 objective lens. Positive cells per field were counted.

### Preparation and Handling of DATS/ Wortmannin/LY294002

For in vivo experiments, DATS was dissolved in 100% DMSO and diluted to a dosage of 100  $\mu$ g/kg per day with sterile saline. We intraperitoneally injected DATS (with/without wortmannin, 1 mg/kg per day) for 10 days after lymphedema surgery.<sup>13</sup> For in vitro experiments, DATS (in DMSO) and a reduced form of L-glutathione-SH (GSH) were diluted to concentrations of 10 or 100  $\mu$ mol/L and 2 mmol/L, respectively, with endothelial cell growth basal medium (EBM-2; Lonza).<sup>13</sup> In some experiments, wortmannin (10 nmol/L) or LY294002 (50  $\mu$ mol/L) was added into the medium.<sup>13,18</sup>

### Measurement of H<sub>2</sub>S

Free H<sub>2</sub>S levels in the tail tissues and the serum samples from lymphedema mice at POD 7 were measured by using an OxiSelect Free Hydrogen Sulfide Gas Assay Kit (Cell Biolabs). This kit was also used to measure H<sub>2</sub>S levels in cell lysates from human lymphatic microvascular endothelial cells, treated with DATS and GSH, following the manufacturer's instructions.

### Cell Culture

Lymphatic endothelial cells (LECs) (human lymphatic microvascular endothelial cells) were purchased from Lonza. Cells were maintained in with Microvascular Endothelial Cell Growth Medium-2 Bullet Kit (EGM-2MV; Lonza).<sup>17</sup>

### Tube Formation Assay

LECs were cultured in EGM-2MV until 90% confluency; the culture medium was then changed to EBM-2 with 0.5% FBS for serum starvation. After overnight starvation, the cells were reseeded onto a 6-well plate coated with Matrigel (Becton Dickinson, Bedford, MA) at  $2 \times 10^4$  cells per well in EBM-2 with 0.5% FBS medium.<sup>22</sup> The cells were incubated at 37 °C for 6 hours with DATS or vehicle, and morphological changes of LECs were microscopically analyzed in 3 different fields per well. Tube formation was assessed by the average of total tube lengths formed in the 3 fields per sample using Image J software (version 1.51).<sup>22</sup>

### Proliferation Assay

Cells were cultured on a 96-well tissue culture plate, stimulated with DATS, and incubated with the water soluble tetrazolium salts-1 (WST-1) reagent in the Premix WST-1 Cell Proliferation Assay System (Takara Bio) for 6 hours,<sup>20,22</sup> using a scanning multiwell spectrophotometer (440nm; reference, 600nm). The absorbance at 440nm (with reference at 600nm) was measured using a scanning multiwell spectrophotometer, which correlates to the viable cell numbers.

### Migration Assay

Cell migration assay was performed using 3-mm pore size Costar transwell migration chambers (Corning) in 24-well plates. LECs ( $4 \times 10^4$  cells/100  $\mu$ L) in EBM-2 with 0.5% FBS and DATS or vehicle were seeded on the top of the chamber membrane. One-tenth of the concentration of EGM-2MV was placed in the lower chamber wells, and the cells were incubated for 8 hours.<sup>22</sup> Cells were then fixed with 3% paraformaldehyde for 15 minutes at room temperature and stained with 0.1% 4',6-diamidino-2-phenylindole for 3 minutes. The stain was rinsed off thoroughly with PBS. Cells that remained on top of the migration chamber were

removed by gentle swabbing using a cotton tip, and the stained cells that adhered to the bottom of the chamber membrane were counted. The numbers of cells in 5 random fields at  $\times 200$  magnification for each migration chamber membrane were counted.

### Western Blot Analysis

Tail samples collected from each experimental group at POD 7 were homogenized, and lysates were prepared for Western blot experiments. For in vitro study, LECs were collected at 30 minutes posttreatment with DATS and GSH, homogenized, and cell lysates were prepared.<sup>13</sup> Western blot analysis was performed as previously described, using antibodies against phospho-Akt (Akt-P<sup>Ser473</sup>; CST; number 4060S, 1:2000), total-Akt (CST; number 9272S, 1:1000), prospero homeobox protein 1 (PROX1) (CST; number 14963, 1:1000), phospho-Erk1/2 (p44/42 MAPK) (CST; number 4370, 1:1000), total-Erk (CST; number 4695, 1:1000), Glyceraldehyde-3-phosphate dehydrogenase (CST; number 2118S, 1:1000), and  $\beta$ -actin (CST; number 3700S, 1:1000).<sup>18,23</sup>

### Isolation of RNA and Real-Time Reverse Transcriptase–Polymerase Chain Reaction

RNA was isolated by the RNeasy Micro Kit according to the manufacturer's instructions (Qiagen).<sup>22</sup> Reverse transcription was performed with 1  $\mu$ g total RNA with ReverTra Ace quantitative polymerase chain reaction RT Master Mix (Toyobo) supplemented with DNase treatment.<sup>22</sup> Real-time reverse transcriptase–polymerase chain reaction analysis of the vascular endothelial growth factor-C (VEGF-C), vascular endothelial growth factor receptor 3 (VEGFR3), and GAPDH was performed on C1000 Thermal Cycler (Bio-Rad) using SYBR Green I and the following conditions: 95 °C for 10 minutes followed by 40 cycles at 95 °C for 15 seconds and 60 °C for 45 seconds.<sup>22</sup> The forward primer for mouse VEGF-C was as follows: 5'- AACGTGTCCAAGAAATCAGCC -3';

the reverse primer: 5'- AGTCCTCTCCCGCAGTAATCC -3'. The forward primer for human VEGFR3 was as follows: 5'- CCTGAAGAAGATCGCTGTTC -3'; the reverse primer: 5'- GAGAGCTGGTTCCTGGAGAT-3'. The forward primer for mouse GAPDH was as follows: 5'- ATGGTGAAGGTCGGTGTG -3'; the reverse primer: 5'- CACATTGGGGGTAGGAACAC -3'. The forward primer for human GAPDH was as follows: 5'- TGGAGAATGAGAGGTGGGATG -3'; the reverse primer: 5'- GAGCTTCACGTTCTTGTATCTGT -3'.

### VEGF-C Measurements

The levels of VEGF-C were evaluated in the cell lysates of LECs using an ELISA kit (Human VEGF-C Quantikine ELISA Kit, number DVECO0; R&D Systems), according to the manufacturer's instructions.

### Statistical Analysis

All data are expressed as mean $\pm$ SEM. A Shapiro-Wilk normality test was performed to evaluate data distribution. Normally distributed data with 1 variable were analyzed by the unpaired Student *t* test to evaluate the statistical significance between the 2 groups. One-way ANOVA, along with Tukey post hoc test, were used for 3 or more groups. We also used a 2-way repeated-measures ANOVA (Sidak post hoc tests) to assess the changes over time. Nonnormally distributed data were analyzed by 2-tailed Mann-Whitney *U* test between 2 groups. GraphPad Prism software version 8.0 (GraphPad Software) was used. Values of  $P < 0.05$  were considered statistically significant.<sup>21,22</sup>

## RESULTS

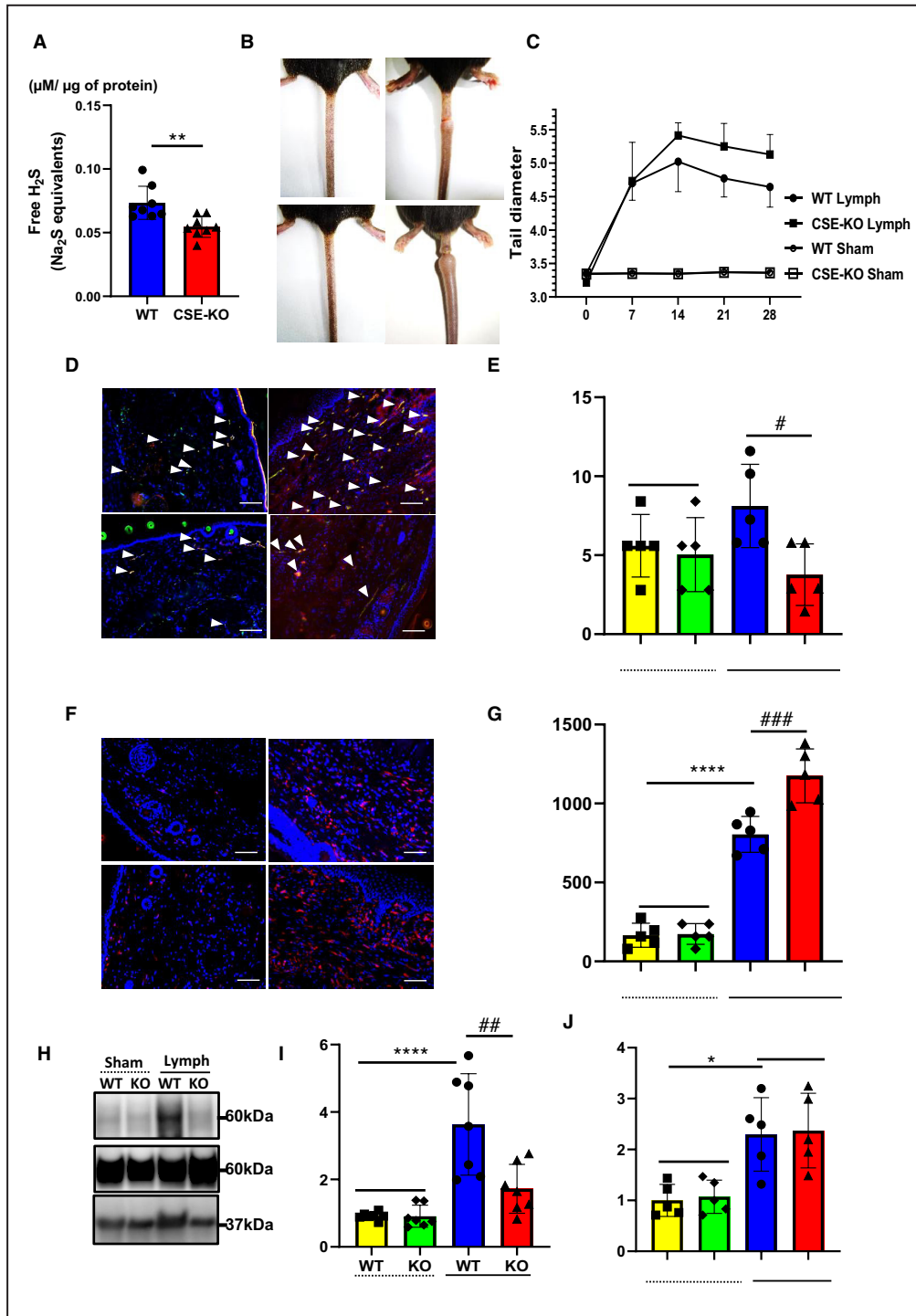
### H<sub>2</sub>S Deficiency Exacerbates Lymphedema After the Ablation of Tail Lymphatic Vessels

To determine if endogenous H<sub>2</sub>S modulates lymphedema, we subjected CSE-KO and WT mice to the

#### Figure 1. CSE deletion attenuates reparative lymphangiogenesis and deteriorates lymphedema after the ablation of tail lymphatic vessels.

**A**, Free H<sub>2</sub>S levels in tail tissues of WT and CSE-KO mice. \*\* $P < 0.01$  vs WT by unpaired Student *t* test. **B**, Representative pictures of murine tail lymphedema models. **C**, Changes in the tail diameters after the surgery. Data are mean $\pm$ SEM (n=5 for WT-Sham; n=5 for CSE-KO-Sham; n=7 for WT-Lymphedema; n=6 for CSE-KO-Lymph). \* $P < 0.05$  vs the respective WT-Lymph by 2-way ANOVA and Sidak's post hoc tests. **D**, Representative immunostaining images with anti-LYVE-1 (green) and anti-podoplanin (red) antibodies at disconnection sites in lymphedema tail sections. White arrowheads indicate LYVE-1/podoplanin double-positive cells. **E**, Quantitative analysis of lymphatic capillary density (LYVE-1/podoplanin double-positive cells). Bars: 100  $\mu$ m. Data are mean $\pm$ SEM. \* $P < 0.05$  vs WT-Lymph by 1-way ANOVA and Tukey post hoc tests. **F**, Representative immunostaining images with anti-F4/80 (red) at distal sites in lymphedema tail sections. **G**, Quantitative analysis of F4/80<sup>+</sup> cells. Bars: 100  $\mu$ m. Data are mean $\pm$ SEM. \*\*\*\* $P < 0.0001$  vs WT-Sham and ### $P = 0.0005$  vs WT-Lymph by 1-way ANOVA and Tukey post hoc tests. **H**, Representative immunoblots against phospho-Akt (p-Akt)<sup>Ser473</sup>, total Akt (t-Akt), and GAPDH (as loading controls). **I**, Quantitative analysis of immunoblots. Data are mean $\pm$ SEM (n=7 each). \*\*\*\* $P < 0.0001$  vs WT-Sham and ## $P < 0.001$  vs CSE-KO-Lymph by 1-way ANOVA and Tukey post hoc tests. **J**, The expression of mRNA VEGF-C in lymphedema tail. Data are mean $\pm$ SEM (n=5 each). \* $P < 0.05$  vs WT-Sham by 1-way ANOVA and Tukey post hoc tests. . Akt indicates protein kinase B; CSE, cystathionine  $\gamma$ -lyase; DAPI, 4',6'-diamidino-2-phenylindole; H<sub>2</sub>S, hydrogen sulfide; KO, knockout; LYVE, lymphatic vessel endothelial hyaluronan receptor 1; mRNA, messenger RNA; N.S., not significant; VEGF-C, vascular endothelial growth factor-C; and WT, wild-type.





ablation of the tail surface lymphatic network. At POD 7, free H<sub>2</sub>S levels were 25.5% lower in the lymphedema tails of CSE-KO mice than those of WT mice (Figure 1A). At POD 21, lymphedema was much more apparent in the tails of CSE-KO mice (Figure 1B). Lymphedema (as evaluated by tail diameters) was significantly induced within a few days after the surgery, most apparent around POD 14, and then slightly remitted by POD 28 in both CSE-KO and WT mice.

However, CSE-KO mice exhibited more severe lymphedema than that in WT mice (Figure 1B and 1C). Because the inhibition of reparative lymphangiogenesis at the sites of lymphatic dysfunction is associated with the deterioration of lymphedema, we assessed the lymphatic capillary density by immunostaining with LEC markers, LYVE-1 (green) and podoplanin (red), in the tail sections (Figure 1D). Quantitative analysis of LYVE-1/podoplanin double-positive cells demonstrated that

lymphatic capillary density in lymphedema tails at POD 28 was 53.6% lower in CSE-KO mice than that in WT mice (Figure 1E). Accumulation of local macrophages detected as F4/80 positive cells increased in the edematous tissue of CSE-KO mice compared with WT mice (Figure 1F and 1G). Phosphoinositide 3'-kinase (PI3K)/Akt signaling is known to regulate lymphangiogenesis under pathological conditions.<sup>24</sup> Our analysis revealed that Akt phosphorylation (at Ser473) levels were highly upregulated in the lymphedema tails of WT mice but not in those of CSE-KO mice (Figure 1H and 1I). However, VEGF-C expression was not downregulated in CSE-KO mice compared with WT mice in lymphedema tissue (Figure 1J).

### DATS Treatment Enhances H<sub>2</sub>S Levels to Promote Reparative Lymphangiogenesis and Improves Lymphedema In Vivo

Next, we investigated whether H<sub>2</sub>S could modulate lymphedema using the H<sub>2</sub>S donor DATS. DATS treatment (100 µg/kg per day) increased free H<sub>2</sub>S levels in blood circulation (Figure 2A), and more markedly, in lymphedema tail tissues (Figure 2B). Compared with the (vehicle) control mice, DATS-treated mice showed significant improvements in lymphedema (at POD 21 and POD 28) (Figure 2C and 2D). Interestingly, DATS treatment also improved lymphedema in CSE-deficient lymphedema mice (Figures S1A and S1B). Immunostaining with LEC markers revealed the increased LEC density in injured tissues with DATS treatment (Figures 2E and 2F). In addition, the lymphatic vessels distal to the skin incision were markedly dilated (for the congestion of lymphatic fluids) in a nontreated control group, whereas dilatation was not evident in the DATS-treated group (Figures 2G and 2H), suggesting the satisfactory drainage of lymphatic fluid in this group. Furthermore, F4/80 staining of tail sections revealed that macrophages infiltrated the subcutaneous tissues of lymphedema in the control animals, which was ameliorated by DATS treatment (Figure 2I and 2J).

Although phosphorylation of Akt was augmented by DATS treatment after lymphatic ablation (Figures 2K and 2L), VEGF-C expression was not changed between those 2 groups (Figure 2M).

### Addition of DATS Augments Lymphangiogenesis In Vitro

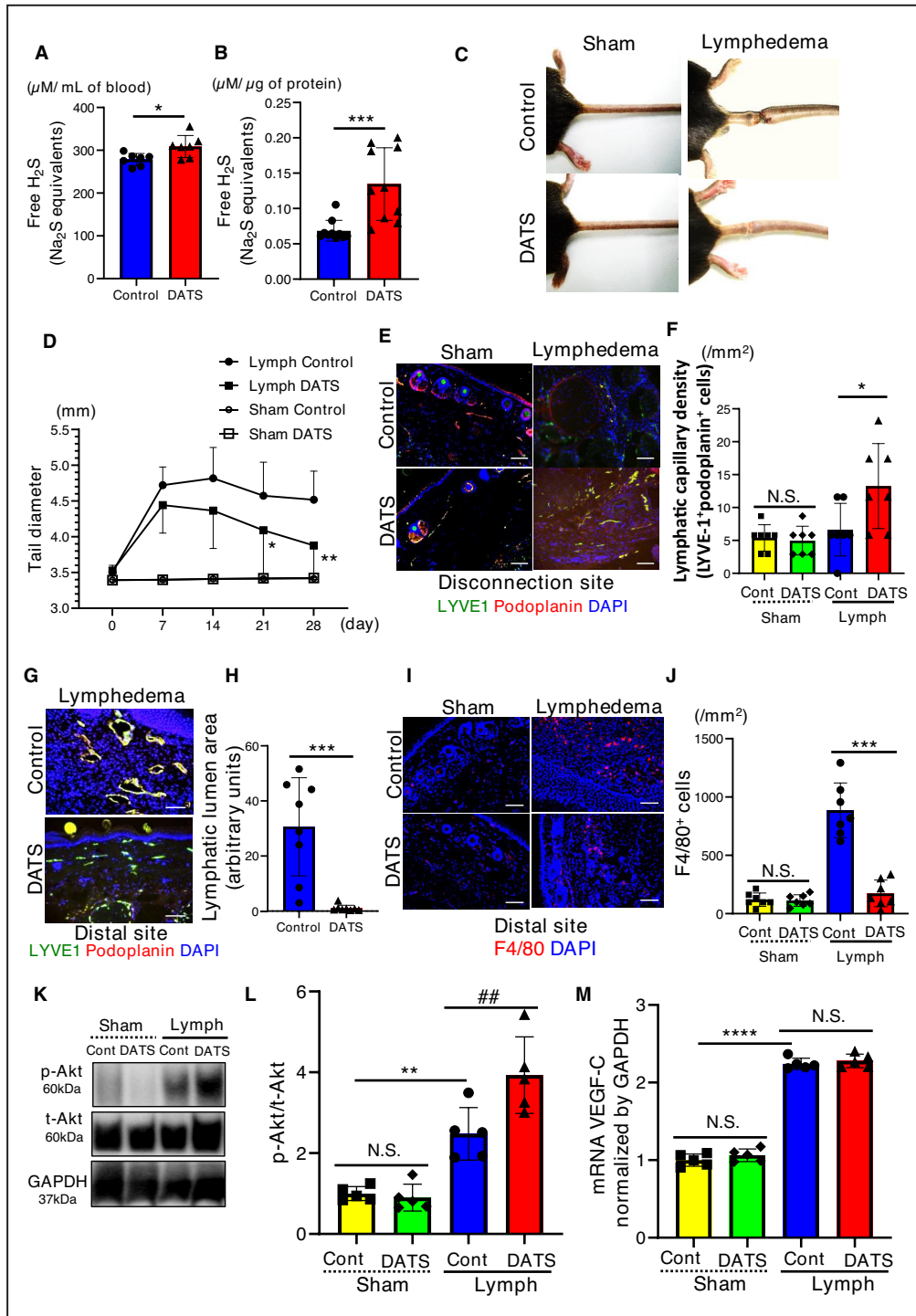
DATS treatment (100 µmol/L) also increased free H<sub>2</sub>S levels in LECs (Figure 3A). In addition, DATS augmented the proliferation of LECs in a dose-dependent manner (Figure 3B) as well as differentiation into a capillary-like structure (Figure 3C). Quantitative analysis revealed that DATS induced 1.82 times increase in total tube length (Figure 3D). DATS treatment upregulated Akt phosphorylation in LECs in a concentration-dependent manner (Figure 3E and 3F), and PROX1 was also upregulated by DATS in the same manner (Figure 3G). VEGF-C levels and VEGFR3 expression in LECs were not changed after DATS treatment (Figure 3H and Figure S2A). Furthermore, DATS also upregulated Akt phosphorylation in LECs in a time-dependent manner (Figure 3I and 3J), followed by PROX1 upregulations (Figure 3K).

### Akt Signaling Is Crucial for DATS-Induced Responses in LECs

As noted, PI3K/Akt signaling is associated with the regulation of lymphangiogenesis under pathological conditions. Therefore, we further investigated the role of PI3K/Akt in mediating the DATS-induced proliferation of LECs. For these experiments, LECs were treated with DATS in the presence or absence of the PI3K inhibitor, wortmannin. Western blot analysis demonstrated that wortmannin negated the DATS-induced phosphorylation of Akt (Figure 4A and 4B), as well as the DATS-induced migration and proliferation of LECs (Figure 4C and 4E). In addition, LY294002 also demonstrated that proliferation ability and migration ability in LECs were reduced by the inhibition of PI3K-Akt signaling in DATS-induced lymphangiogenesis (Figures S3). Collectively, these results indicate that

#### Figure 2. DATS augments lymphangiogenesis in murine tail lymphedema.

**A and B**, Free H<sub>2</sub>S levels in blood (**A**) and tail tissues (**B**) in DATS-treated and (vehicle-treated) control (Cont) groups. Data are mean±SEM (n=7 each). \**P*<0.05 and \*\*\**P*<0.001 vs control by 2-tailed Mann-Whitney *U* test. **C**, Representative pictures of murine tail lymphedema models. **D**, Changes in tail diameters after the surgery. Data are mean±SEM (n=10 for Sham-[Vehicle] Control; n=10 for Sham-DATS; n=11 for Lymph-[Vehicle] Control; n=10 for Lymph-DATS). \**P*<0.05 and \*\**P*<0.01 vs the respective WT by 2-way ANOVA and Sidak post hoc tests. **E**, Representative immunostaining images with anti-LYVE-1 (green) and anti-podoplanin (red) antibodies at the disconnection sites of lymphedema tail sections. **F**, Quantitative analysis of lymphatic capillary density (LYVE-1/podoplanin double-positive cells). Bars: 100 µm. \**P*<0.05 vs Lymph-Control by 1-way ANOVA and Tukey post hoc tests. **G**, Representative immunostaining images with anti-LYVE-1 (green) and anti-podoplanin (red) at distal sites of lymphedema tail sections. **H**, Quantitative analysis of lymphatic lumen areas. Bars: 100 µm. \*\*\**P*<0.001 vs control by 2-tailed Mann-Whitney *U* test. **I**, Representative immunostaining images with anti-F4/80 (red) at the distal sites of lymphedema tail sections. **J**, Quantitative analysis of F4/80-positive cells. Bars: 100 µm. \*\*\**P*<0.001 vs Lymph-Control by 1-way ANOVA and Tukey post hoc tests. **K**, Representative immunoblots of p-Akt, Akt, and GAPDH. **L**, Quantitative analysis of immunoblots. Data are mean±SEM (n=5 each). \*\**P*<0.01 vs Sham-Control and ##*P*<0.01 vs Lymph-DATS by 1-way ANOVA and Tukey post hoc tests. **M**, The expression of mRNA VEGF-C in lymphedema tail with/without DATS treatment. Data are mean±SEM (n=5 each). \*\*\*\**P*<0.0001 vs Sham-Control by 1-way ANOVA and Tukey post hoc tests. Akt indicates protein kinase B; Cont, control; DAPI, 4',6-diamidino-2-phenylindole; DATS, diallyl trisulfide; H<sub>2</sub>S, hydrogen sulfide; LYVE-1, lymphatic vessel endothelial hyaluronan receptor 1; mRNA, messenger RNA; N.S., not significant; p-Akt, phospho-Akt; t-Akt, total Akt; VEGF-C, vascular endothelial growth factor-C; and WT, wild-type.



PI3K-Akt signaling is required for LEC responses to DATS in vitro.

### Role of Akt Signaling in Lymphangiogenic Responses to DATS In Vivo

Finally, we examined whether Akt is required for the in vivo activity of DATS on lymphedema. For these experiments, we intraperitoneally injected wortmannin or vehicle to

DATS-treated lymphedema mice. Wortmannin was found to negate DATS-induced improvements in lymphedema (Figure 5A and 5B), lymphangiogenesis (Figures 5C and 5D), and macrophages infiltration (Figures 5E and 5F). Wortmannin treatment canceled DATS-induced phosphorylation of Akt in lymphedema tissues (Figures 5G and 5H). These results collectively suggest that the in vivo therapeutic effects of DATS on lymphedema are, at least in part, dependent on its ability to modulate Akt activity.

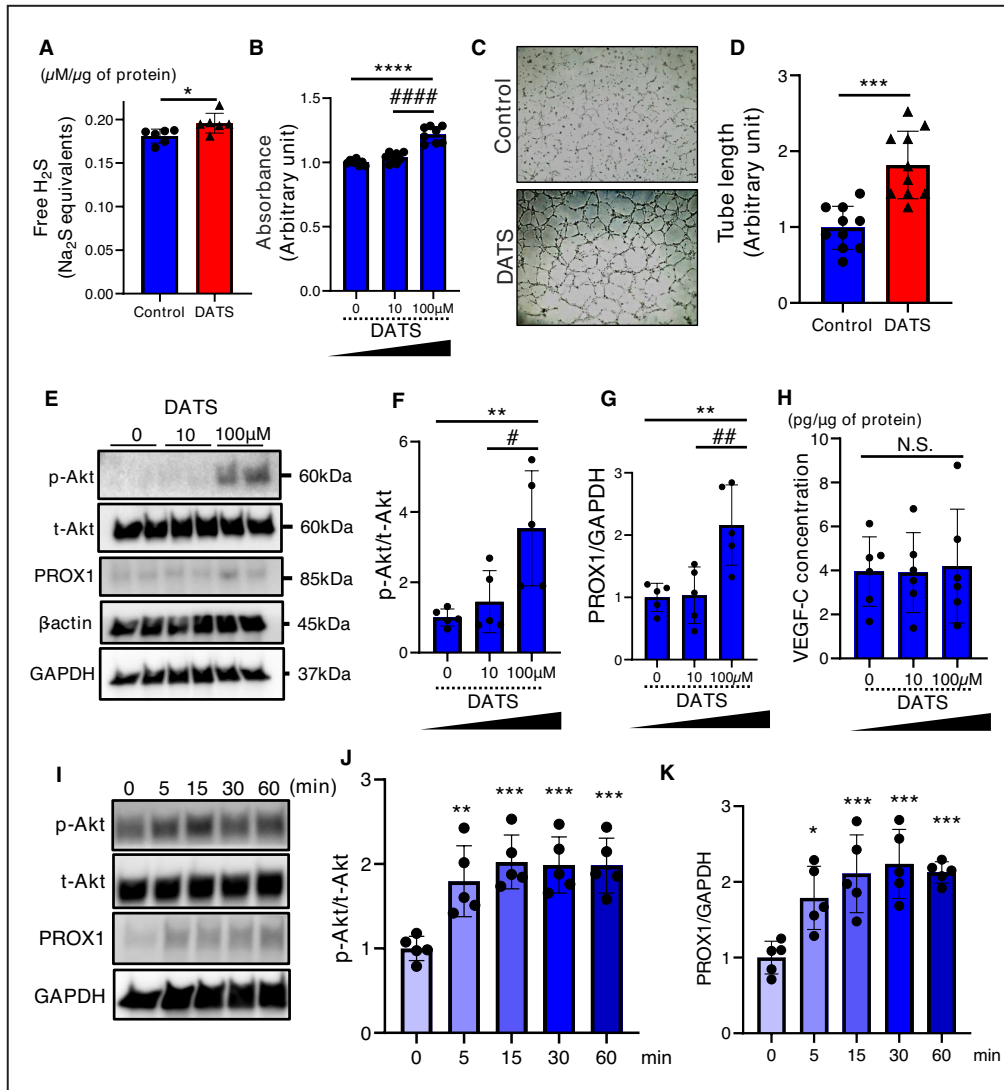


**Figure 3. DATS promotes lymphatic endothelial cell proliferation, tube-like structure formation, and Akt phosphorylation.**

**A**, Free  $H_2S$  levels in LECs treated with/without DATS. Data are mean $\pm$ SEM (n=6 each). \* $P$ <0.05 vs control by Student  $t$  test. **B**, WST-1 proliferation assay of LECs in response to DATS (n=7 each). \*\*\*\* $P$ <0.0001 vs 0 $\mu$ mol/L, #### $P$ <0.0001 vs 10 $\mu$ mol/L by 1-way ANOVA and Tukey post hoc tests. **C**, Representative images of DATS-induced tube formation in LECs. **D**, Quantitative analysis of total tube lengths. Data are mean $\pm$ SEM (n=10 each). \*\*\* $P$ <0.001 vs control by Student  $t$  test. **E**, Representative immunoblots of p-Akt, Akt, PROX1,  $\beta$ -Actin, and GAPDH after DATS treatment. **F**, Quantitative analysis of Akt phosphorylation. Data are mean $\pm$ SEM (n=7 each). \*\* $P$ <0.01 vs 0 $\mu$ mol/L and # $P$ <0.05 vs 10 $\mu$ mol/L by 1-way ANOVA and Tukey post hoc tests. **G**, Quantitative analysis of PROX1. Data are mean $\pm$ SEM (n=5 each). \*\* $P$ <0.01 vs 0 $\mu$ mol/L and ## $P$ <0.01 vs 10 $\mu$ mol/L by 1-way ANOVA and Tukey post hoc tests. **H**, Level of VEGF-C concentration in LECs after DATS treatment detected by an ELISA kit. Data are mean $\pm$ SEM (n=6 for each). **I**, Representative immunoblots of p-Akt, Akt, PROX1, and GAPDH at sequential time points after DATS treatment. **J**, Quantitative analysis of Akt phosphorylation. Data are mean $\pm$ SEM (n=5 each). \*\* $P$ <0.01 and \*\*\* $P$ <0.001 vs 0 minutes by 1-way ANOVA and Tukey post hoc tests. **K**, Quantitative analysis of PROX1. Data are mean $\pm$ SEM (n=5 each). \* $P$ <0.05 and \*\*\* $P$ <0.001 vs 0 minutes by 1-way ANOVA and Tukey post hoc tests. Akt indicates protein kinase B; DATS, diallyl trisulfide;  $H_2S$ , hydrogen sulfide; LECs, lymphatic endothelial cells; N.S., not significant; p-Akt, phospho-Akt; PROX1, prospero homeobox protein-1; t-Akt, total Akt; VEGF-C, vascular endothelial growth factor-C; and WST-1, water soluble tetrazolium salts-1.

## DISCUSSION

The major findings of the present study are as follows: (1) the genetic deletion of CSE in mice caused low  $H_2S$

levels, reduced lymphangiogenesis, and exacerbated lymphedema in a murine model of tail lymphedema. (2) The systemic administration of the  $H_2S$  donor, DATS, to WT mice increased  $H_2S$  levels and enhanced



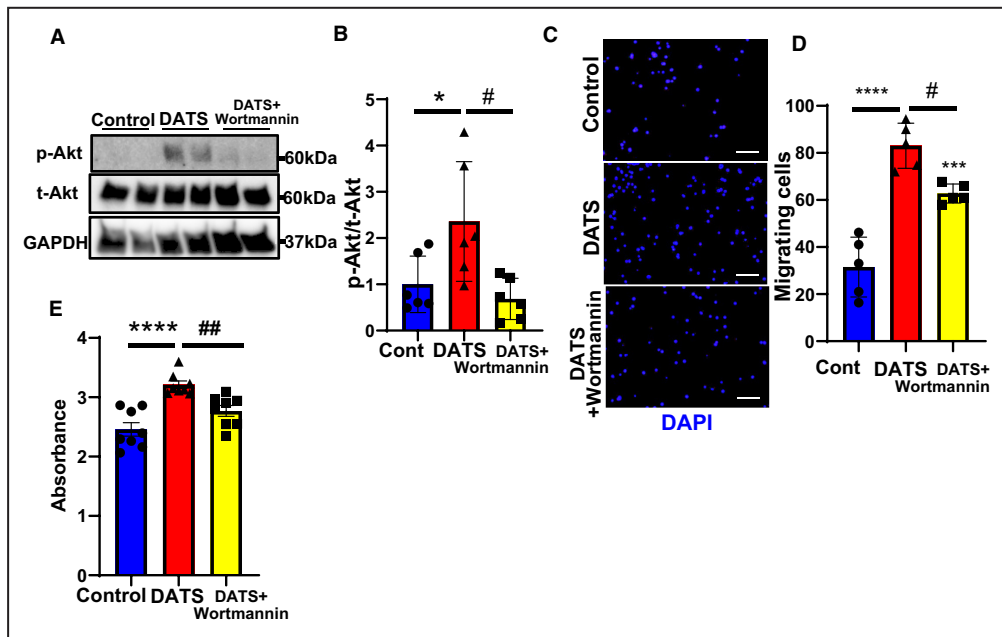


**Figure 4. PI3K/Akt signaling participates in lymphatic vessel responses to DATS in vitro.**

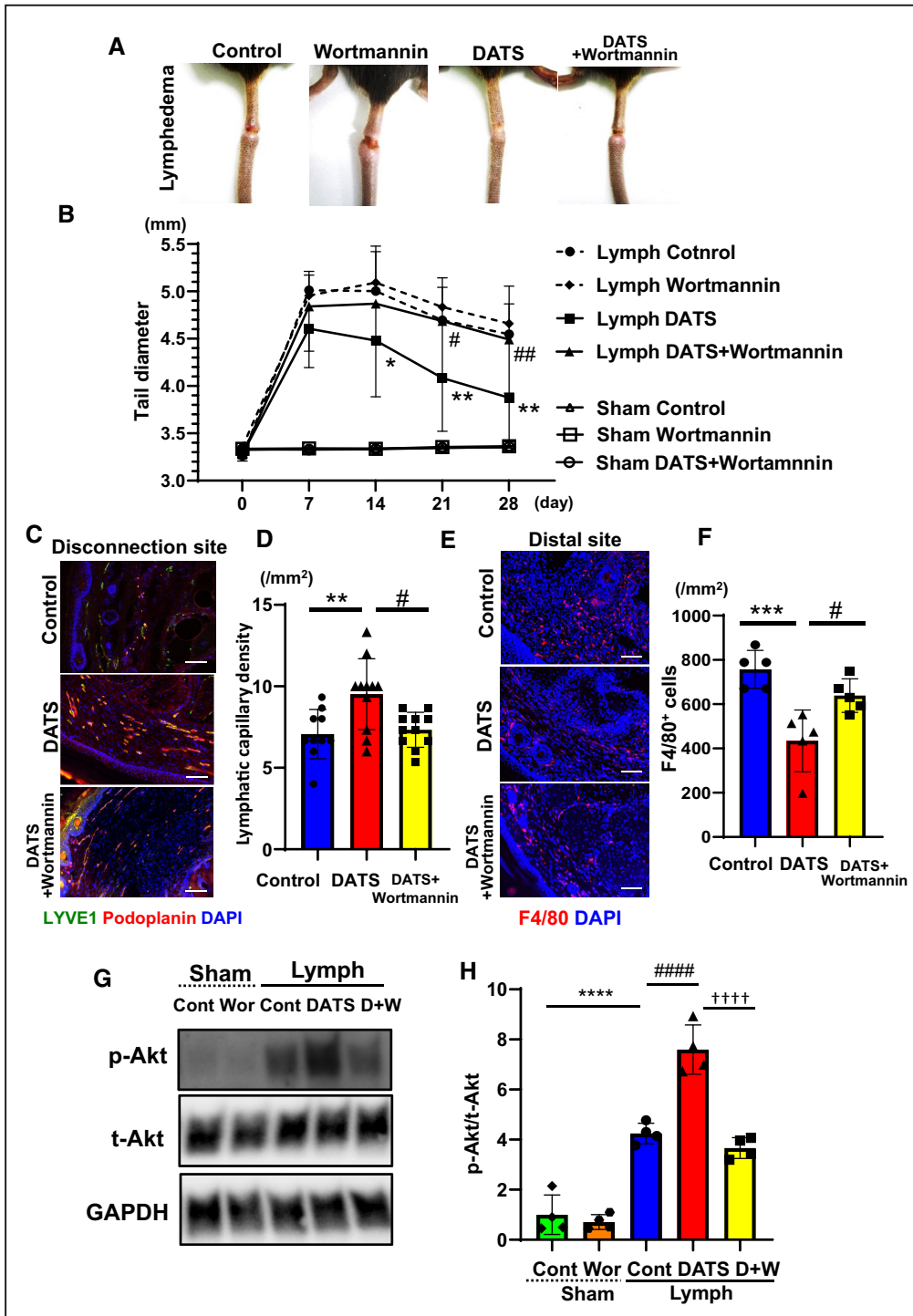
**A**, Representative immunoblots of p-Akt and Akt after DATS treatment without/with wortmannin. **B**, Quantitative analysis of Akt phosphorylation. Data are mean±SEM (n=5 for each). \* $P < 0.05$  vs control and # $P < 0.05$  vs DATS by 1-way ANOVA and Tukey post hoc tests. **C**, Representative images of DAPI-stained migrating cells. Bars: 100  $\mu$ m. **D**, Quantitative analysis of migrating cells. Data are mean±SEM (n=6 for each). \*\*\* $P < 0.001$  and \*\*\*\* $P < 0.0001$  vs control and # $P < 0.05$  vs DATS by 1-way ANOVA and Tukey post hoc tests. **E**, WST-1 proliferation assay of LECs in response to treatments with DATS or DATS+wortmannin (n=8 for each). \*\*\*\* $P < 0.0001$  vs control and ## $P < 0.01$  vs DATS by 1-way ANOVA and Tukey post hoc tests. Akt indicates protein kinase B; Cont, control; DATS, diallyl trisulfide; DAPI, 4',6-diamidino-2-phenylindole; p-Akt, phospho-Akt; PI3K, phosphoinositide 3'-kinase; t-Akt, total Akt; and WST-1, water soluble tetrazolium salts-1.

lymphangiogenesis, with subsequent improvements in lymphedema. (3) DATS treatment enhanced the in vitro proliferation, migration, and tube formation of LECs. (4) Inhibition of the PI3K-Akt signaling pathway partially negated the DATS-mediated lymphangiogenesis, both in vitro and in vivo.

Lymphedema is a pathological condition characterized by excessive interstitial edema of the extremities because of lymphatic insufficiency, resulting in dermatopathological morbidity, such as increased limb girth, fibrosis, inflammation, and abnormal fat deposition.<sup>2</sup> Although it is initially reversible, lymphedema often develops into a chronic, irreversible, lifelong complication. In recent studies,  $\approx 1$  out of 7 patients treated for cancer is reported to experience a certain state of lymphedema, and the prevalence is expected to increase in proportion to the extended life expectancy of cancer survivors.<sup>2</sup> However, the disease onset is difficult to control because it often manifests several years after surgery. Treatment options include conservative physical strategies, such as combined decongestive therapy (eg, compression garments), intermittent pneumatic compression, and newer surgical interventions, including liposuction for end-stage disease, all of which remain coping strategies.<sup>1</sup> In contrast, therapeutic lymphangiogenesis reconstructs the

lymphatic network once it has been dissected, and is expected to be a fundamental treatment for secondary lymphedema.<sup>3,25</sup>

Lymphatic vessels run through organs in the whole body, like blood vessels, and drain lymph fluid from intercellular spaces to regulate tissue edema, inflammatory cell infiltrations, levels of proteins, and lipids.<sup>26</sup> Therefore, they play a pivotal role in maintaining tissue homeostasis and in monitoring various immune reactions.<sup>26</sup> In contrast, recent findings suggest that lymphatic vessels play an important role in the pathogenesis of multiple inflammatory diseases and in the regeneration process of damaged tissues.<sup>27</sup> For instance, it is known that the insufficient formation or dysfunction of lymphatic vessels exacerbates pathological conditions.<sup>19,21,28</sup> Conversely, lymphangiogenesis can accelerate wound healing and subsequently maintain organ functions by improving inflammation and inhibiting fibrosis during the extreme phase of pathological conditions.<sup>19,21,29,30</sup> Thus, therapeutic lymphangiogenesis is a promising strategy for promoting reparative lymphangiogenesis of endogenous ecological responses to improve pathological conditions, such as ischemic heart disease, critical ischemic limb, and lymphedema. The supplementation of lymphangiogenesis-promoting factors or cell



Downloaded from <http://ahajournals.org> by on November 7, 2022

transplantation to promote lymphangiogenesis protects from tissue damage and augments the tissue regeneration process.<sup>17-19,21</sup>

H<sub>2</sub>S has been reported to promote angiogenesis in various models including the Matrigel plugs assay, myocardial ischemia-reperfusion injury, and hindlimb ischemia models.<sup>13,31-33</sup> However, little is known about the effect of H<sub>2</sub>S on lymphangiogenesis. To our knowledge, the present study is the first to provide novel

evidence that H<sub>2</sub>S could promote lymphangiogenesis, both in vivo and in vitro.

H<sub>2</sub>S is primarily synthesized by enzymatic methods. Three enzymes, cystathionine β-synthase, CSE, and 3-metacaptopyrivate sulfotransferase, perform the synthesis.<sup>7</sup> CSE, in particular, is found mainly in the cardiovascular system and plays an important role in H<sub>2</sub>S-induced cardiovascular protection. Both cystathionine β-synthase and CSE interact with L-cysteine to

**Figure 5. Inhibition of PI3K/Akt pathway partially impedes DATS-induced lymphangiogenesis in vivo.**

**A**, Representative pictures of tail lymphedema in mice administered with Vehicle, DATS, Wortmannin, and DATS+Wortmannin in lymphedema models. **B**, Changes in tail diameters after the surgery. Data are mean±SEM (n=9 for Lymph-Control, Lymph-Wortmannin, Lymph-DATS, and Lymph-DATS+Wortmannin; n=5 for Sham-[Vehicle] Control, Sham-Wortmannin, and Sham-DATS+Wortmannin). \**P*<0.05 and \*\**P*<0.01 vs respective Lymph-(Vehicle) Control; #*P*<0.05 and ##*P*<0.01 vs respective Lymph-DATS by 2-way ANOVA and Sidak post hoc tests. **C**, Representative immunostaining images with anti-LYVE-1 (green) and anti-podoplanin (red) antibodies at the lymphatic disconnection sites in lymphedema tails. **D**, Quantitative analysis of lymphatic capillary density (LYVE-1/podoplanin double-positive cells). Bars: 100µm. Data are mean±SEM (n=11 for each). \*\**P*<0.01 vs control and #*P*<0.05 vs DATS samples by 1-way ANOVA and Tukey post hoc tests. **E**, Representative immunostaining images with anti-F4/80 (red) at distal sites of lymphedema tail sections. **F**, Quantitative analysis of F4/80-positive cells. Bars: 100µm. \*\*\**P*<0.001 vs control and #*P*<0.05 vs DATS by 1-way ANOVA and Tukey post hoc tests. **G**, Representative immunoblots of p-Akt, Akt, and GAPDH after DATS without/with wortmannin treatment. **H**, Quantitative analysis of Akt phosphorylation. Data are mean±SEM (n=4 each). \*\*\*\**P*<0.0001 vs Sham-Control, ####*P*<0.0001 vs Lymph-Control, and ++++*P*<0.0001 vs Lymph-DATS by 1-way ANOVA and Tukey post hoc tests. Akt indicates protein kinase B; Cont, control; DAPI, 4,6-diamidino-2-phenylindole; DATS, diallyl trisulfide; D+W, DATS+Wortmannin; LYVE-1, lymphatic vessel endothelial hyaluronan receptor 1; p-Akt, phospho-Akt; PI3K, phosphoinositide 3'-kinase; t-Akt, total Akt; and Wor, Wortmannin.

produce H<sub>2</sub>S; L-serine and ammonium are produced as by-products, which are assumed to influence H<sub>2</sub>S regulation throughout body tissues.<sup>7</sup> Here, we demonstrated that CSE-KO mice displayed impairment of reparative lymphangiogenesis, resulting in worsened lymphedema. In addition, DATS-induced increase in H<sub>2</sub>S levels can elicit lymphangiogenesis for the amelioration of lymphedema. These findings suggest that H<sub>2</sub>S acts as an endogenous enhancer of lymphatic vessel formation in response to tissue injury and exerts a salutary action on the lymphatic vasculature. DATS is an organic polysulfide found in garlic oil; it liberates H<sub>2</sub>S under physiological conditions.<sup>8</sup> In the current study, the chronic administration of DATS protected against the adverse remodeling associated with lymphatic injury by increasing circulating and local sulfide levels. Specifically, we found that DATS treatment augmented reparative lymphangiogenesis, and attenuated the development of interstitial fluid accumulation and local inflammation, and thereby secondary lymphedema.

H<sub>2</sub>S modulates the PI3K/Akt pathway in multiple cells.<sup>34–37</sup> For instance, H<sub>2</sub>S exerts cardioprotection against ischemia–reperfusion injury and against pressure-overload heart failure models via Akt phosphorylation.<sup>38,39</sup> H<sub>2</sub>S has also been reported to modulate PI3K-Akt signaling in vascular smooth muscle cells against high glucose-induced apoptosis.<sup>40</sup> H<sub>2</sub>S also activates the PI3K/Akt signaling and exerts its function in vascular endothelial cells.<sup>31,39,41,42</sup> In addition, DATS was reported to activate the PI3K/Akt signaling, which plays an important role in the process of reparative angiogenesis.<sup>13,43</sup> To our knowledge, the present study is the first to demonstrate that H<sub>2</sub>S activates the PI3K/Akt pathway in LECs, similar to other cell types.

The Akt pathway regulates various cellular functions via phosphorylation.<sup>24</sup> For example, it is well known that Akt activates mechanistic/mammalian target of rapamycin complex 1 by inhibiting tuberous sclerosis complex 2 and promotes cell proliferation by initiating translation and ribosome biogenesis.<sup>44,45</sup> Akt can also inactivate cyclin-dependent kinase inhibitors such as p21 and

p27 and regulate the promotion of cell cycle progression.<sup>46</sup> In addition, Akt-related signals contribute to the augmentation of migration and tube formation ability in endothelial cells and promote angiogenesis in multiple ways. Therefore, it has been suggested that the PI3K/Akt signaling also plays an important role in lymphatic vessel architecture (including lymphangiogenesis) by regulating these downstream signals in LECs.<sup>47,48</sup> In our current study, blockading for H<sub>2</sub>S-induced Akt phosphorylation inhibited proliferative and migratory ability in LECs. Furthermore, in vivo validation in a lymphedema model showed that the lymphangiogenic effect, and therapeutic effect against lymphedema, of H<sub>2</sub>S was attenuated in the PI3K inhibitor-treated group, resulting in an attenuation of the effect on lymphedema attenuation. In summary, our findings suggest that the underlying mechanism of the H<sub>2</sub>S-induced lymphangiogenesis was mediated, at least in part, via the PI3K/Akt pathway.

Our data demonstrated that H<sub>2</sub>S did not modulate the VEGF-C levels themselves in lymphedema in the CSE-deficiency mice or the DATS-treated mice. In vascular endothelial cells, H<sub>2</sub>S is known to promote angiogenesis by sulfhydration and stabilizing the transcription factor specificity protein 1 (Sp1), followed by enhancing vascular endothelial growth factor receptor 2 (VEGFR2) signaling.<sup>37,49,50</sup> It has also been reported that H<sub>2</sub>S acts on the ATP-sensitive potassium channel to promote angiogenesis. Collectively, although our experiments showed that H<sub>2</sub>S did not regulate VEGFC expression in the lymphedema model, it is possible that H<sub>2</sub>S may enhance VEGFR3 signaling by a similar mechanism and activate the PI3K/Akt pathway resulting in the PROX1 upregulation in lymphatic endothelial cells, and promoting lymphangiogenesis in terms of proliferation, and tube formation of LECs. Further experiments are needed in the future.

Our tail lymphedema models were well established and used to test the therapeutic lymphangiogenesis to date.<sup>17,18</sup> Recently, other modified versions of the tail lymphedema model leaving an intact collecting vessel have been reported for analysis of functional changes during disease progression.<sup>51</sup> We need to test the

effect of H<sub>2</sub>S on this new model and evaluate if the functional lymphatic vessels were constructed by therapeutic lymphangiogenesis for future studies.

In conclusion, H<sub>2</sub>S promotes reparative lymphangiogenesis and ameliorates secondary lymphedema, at least in part via PI3K/Akt signaling. In addition, therapeutic lymphangiogenesis using H<sub>2</sub>S donors like DATS could be a therapeutic strategy for refractory secondary lymphedema.

## ARTICLE INFORMATION

Received May 20, 2022; accepted September 19, 2022.

### Affiliations

Department of Cardiology, Nagoya University Graduate School of Medicine, Nagoya, Japan (J.S., Y.S., T.H., Y.C., Z.P., K.T., S.N., T.M.); Department of Advanced Cardiovascular Therapeutics, Nagoya University Graduate School of Medicine, Nagoya, Japan (R.S.); Laboratory of Health Chemistry, Showa Pharmaceutical University, Machida, Tokyo, Japan (I.I.); and Department of Surgery, Division of Cardiothoracic Surgery, Carlyle Fraser Heart Center, Emory University School of Medicine, Atlanta, GA (J.W.C.).

### Acknowledgments

The authors are grateful to the staff from the Division of Experimental Animals at the Nagoya University School of Medicine for assisting with animal experiments. We thank Y. Inoue for her technical assistance.

### Sources of Funding

This work was supported by grants (number 17H06745 to Y.S.) from the Ministry of Education, Culture, Sports, Science and Technology of Japan; and a research grant from Mitsubishi Tanabe Pharma Corporation (number MTPS20190601012) to Y.S.

### Disclosures

None.

### Supplemental Material

Figure S1

## REFERENCES

- Rockson SG. Lymphedema after breast cancer treatment. *N Engl J Med*. 2018;379:1937–1944. doi: 10.1056/NEJMcp1803290
- Rockson SG, Keeley V, Kilbreath S, Szuba A, Towers A. Cancer-associated secondary lymphoedema. *Nat Rev Dis Primers*. 2019;5:22. doi: 10.1038/s41572-019-0072-5
- Norrmén C, Tammela T, Petrova TV, Alitalo K. Biological basis of therapeutic lymphangiogenesis. *Circulation*. 2011;123:1335–1351. doi: 10.1161/CIRCULATIONAHA.107.704098
- Kimura H. Signaling molecules: Hydrogen sulfide and polysulfide. *Antioxid Redox Signal*. 2015;22:362–376. doi: 10.1089/ars.2014.5869
- Kimura H. Production and physiological effects of hydrogen sulfide. *Antioxid Redox Signal*. 2014;20:783–793. doi: 10.1089/ars.2013.5309
- Calvert JW, Coetzee WA, Lefer DJ. Novel insights into hydrogen sulfide-mediated cytoprotection. *Antioxid Redox Signal*. 2010;12:1203–1217. doi: 10.1089/ars.2009.2882
- Kolluru GK, Shen X, Bir SC, Kevill CG. Hydrogen sulfide chemical biology: pathophysiological roles and detection. *Nitric Oxide*. 2013;35:5–20. doi: 10.1016/j.niox.2013.07.002
- Bradley JM, Organ CL, Lefer DJ. Garlic-derived organic polysulfides and myocardial protection. *J Nutr*. 2016;146:403S–409S. doi: 10.3945/jn.114.208066
- Kondo K, Bhushan S, King AL, Prabhu SD, Hamid T, Koenig S, Murohara T, Predmore BL, Gojon G Sr, Gojon G Jr, et al. H<sub>2</sub>S protects against pressure overload-induced heart failure via upregulation of endothelial nitric oxide synthase. *Circulation*. 2013;127:1116–1127. doi: 10.1161/CIRCULATIONAHA.112.000855
- Shimizu Y, Nicholson CK, Lambert JP, Barr LA, Kuek N, Herszenhaut D, Tan L, Murohara T, Hansen JM, Husain A, et al. Sodium sulfide attenuates ischemic-induced heart failure by enhancing proteasomal function in an Nrf2-dependent manner. *Circ Heart Fail*. 2016;9:e002368. doi: 10.1161/CIRCHEARTFAILURE.115.002368
- Barr LA, Shimizu Y, Lambert JP, Nicholson CK, Calvert JW. Hydrogen sulfide attenuates high fat diet-induced cardiac dysfunction via the suppression of endoplasmic reticulum stress. *Nitric Oxide*. 2015;46:145–156. doi: 10.1016/j.niox.2014.12.013
- Shimizu Y, Polavarapu R, Eskla KL, Nicholson CK, Koczor CA, Wang R, Lewis W, Shiva S, Lefer DJ, Calvert JW. Hydrogen sulfide regulates cardiac mitochondrial biogenesis via the activation of AMPK. *J Mol Cell Cardiol*. 2018;116:29–40. doi: 10.1016/j.yjmcc.2018.01.011
- Hayashida R, Kondo K, Morita S, Unno K, Shintani S, Shimizu Y, Calvert JW, Shibata R, Murohara T. Diallyl trisulfide augments ischemia-induced angiogenesis via an endothelial nitric oxide synthase-dependent mechanism. *Circ J*. 2017;81:870–878. doi: 10.1253/circj.CJ-16-1097
- Islam KN, Polhemus DJ, Donnarumma E, Brewster LP, Lefer DJ. Hydrogen sulfide levels and nuclear factor-erythroid 2-related factor 2 (NRF2) activity are attenuated in the setting of critical limb ischemia (CLI). *J Am Heart Assoc*. 2015;4:e001986. doi: 10.1161/JAHA.115.001986
- Ishii I, Akahoshi N, Yamada H, Nakano S, Izumi T, Suematsu M. Cystathionine gamma-lyase-deficient mice require dietary cysteine to protect against acute lethal myopathy and oxidative injury. *J Biol Chem*. 2010;285:26358–26368. doi: 10.1074/jbc.M110.147439
- Robinet P, Milewicz DM, Cassis LA, Leeper NJ, Lu HS, Smith JD. Consideration of sex differences in design and reporting of experimental arterial pathology studies—statement from ATVB council. *Arterioscler Thromb Vasc Biol*. 2018;38:292–303. doi: 10.1161/ATVBAHA.117.309524
- Shimizu Y, Shibata R, Shintani S, Ishii M, Murohara T. Therapeutic lymphangiogenesis with implantation of adipose-derived regenerative cells. *J Am Heart Assoc*. 2012;1:e000877. doi: 10.1161/JAHA.112.000877
- Shimizu Y, Shibata R, Ishii M, Ohashi K, Kambara T, Uemura Y, Yuasa D, Kataoka Y, Kihara S, Murohara T, et al. Adiponectin-mediated modulation of lymphatic vessel formation and lymphedema. *J Am Heart Assoc*. 2013;2:e000438. doi: 10.1161/JAHA.113.000438
- Shimizu Y, Polavarapu R, Eskla KL, Pantner Y, Nicholson CK, Ishii M, Brunnhoelzl D, Mauria R, Husain A, Naqvi N, et al. Impact of lymphangiogenesis on cardiac remodeling after ischemia and reperfusion injury. *J Am Heart Assoc*. 2018;7:e009565. doi: 10.1161/JAHA.118.009565
- Suzuki J, Shimizu Y, Tsuzuki K, Pu Z, Narita S, Yamaguchi S, Katagiri T, Iwata E, Masutomi T, Fujikawa Y, et al. No influence on tumor growth by intramuscular injection of adipose-derived regenerative cells: safety evaluation of therapeutic angiogenesis with cell therapy. *Am J Physiol Heart Circ Physiol*. 2021;320:H447–H457. doi: 10.1152/ajpheart.00564.2020
- Pu Z, Shimizu Y, Tsuzuki K, Suzuki J, Hayashida R, Kondo K, Fujikawa Y, Unno K, Ohashi K, Takefuji M, et al. Important role of concomitant lymphangiogenesis for reparative angiogenesis in hindlimb ischemia. *Arterioscler Thromb Vasc Biol*. 2021;41:2006–2018. doi: 10.1161/ATVBAHA.121.316191
- Tsuzuki K, Shimizu Y, Suzuki J, Pu Z, Yamaguchi S, Fujikawa Y, Kato K, Ohashi K, Takefuji M, Bando YK, et al. Adverse effect of circadian rhythm disorder on reparative angiogenesis in hind limb ischemia. *J Am Heart Assoc*. 2021;10:e020896. doi: 10.1161/JAHA.121.020896
- Pantner Y, Polavarapu R, Chin LS, Li L, Shimizu Y, Calvert JW. DJ-1 attenuates the glycation of mitochondrial complex I and complex III in the post-ischemic heart. *Sci Rep*. 2021;11:19408. doi: 10.1038/s41598-021-98722-1
- Bui K, Hong YK. Ras pathways on Prox1 and lymphangiogenesis: insights for therapeutics. *Front Cardiovasc Med*. 2020;7:597374. doi: 10.3389/fcvm.2020.597374
- Saito Y, Nakagami H, Kaneda Y, Morishita R. Lymphedema and therapeutic lymphangiogenesis. *Biomed Res Int*. 2013;2013:804675. doi: 10.1155/2013/804675
- Tammela T, Alitalo K. Lymphangiogenesis: molecular mechanisms and future promise. *Cell*. 2010;140:460–476. doi: 10.1016/j.cell.2010.01.045
- Alitalo K. The lymphatic vasculature in disease. *Nat Med*. 2011;17:1371–1380. doi: 10.1038/nm.2545
- Black LM, Farrell ER, Barwinska D, Osis G, Zmijewska AA, Traylor AM, Esman SK, Bolisetty S, Whipple G, Kamocka MM, et al. VEGFR3 tyrosine kinase inhibition aggravates cisplatin nephrotoxicity. *Am J Physiol Renal Physiol*. 2021;321:F675–F688. doi: 10.1152/ajprenal.00186.2021



29. Hasegawa S, Nakano T, Torisu K, Tsuchimoto A, Eriguchi M, Haruyama N, Masutani K, Tsuruya K, Kitazono T. Vascular endothelial growth factor-C ameliorates renal interstitial fibrosis through lymphangiogenesis in mouse unilateral ureteral obstruction. *Lab Invest*. 2017;97:1439–1452. doi: 10.1038/labinvest.2017.77
30. Nakamoto S, Ito Y, Nishizawa N, Goto T, Kojo K, Kumamoto Y, Watanabe M, Majima M. Lymphangiogenesis and accumulation of reparative macrophages contribute to liver repair after hepatic ischemia-reperfusion injury. *Angiogenesis*. 2020;23:395–410. doi: 10.1007/s10456-020-09718-w
31. Coletta C, Papapetropoulos A, Erdelyi K, Olah G, Modis K, Panopoulos P, Asimakopoulou A, Gero D, Sharina I, Martin E, et al. Hydrogen sulfide and nitric oxide are mutually dependent in the regulation of angiogenesis and endothelium-dependent vasorelaxation. *Proc Natl Acad Sci USA*. 2012;109:9161–9166. doi: 10.1073/pnas.1202916109
32. Polhemus D, Kondo K, Bhushan S, Bir SC, Kevil CG, Murohara T, Lefer DJ, Calvert JW. Hydrogen sulfide attenuates cardiac dysfunction after heart failure via induction of angiogenesis. *Circ Heart Fail*. 2013;6:1077–1086. doi: 10.1161/CIRCHEARTFAILURE.113.000299
33. Yuan S, Yurdagul A Jr, Peretik JM, Alfaidi M, Al Yafeai Z, Pardue S, Kevil CG, Orr AW. Cystathionine gamma-lyase modulates flow-dependent vascular remodeling. *Arterioscler Thromb Vasc Biol*. 2018;38:2126–2136. doi: 10.1161/ATVBAHA.118.311402
34. Li T, Li J, Li T, Zhao Y, Ke H, Wang S, Liu D, Wang Z. L-cysteine provides neuroprotection of hypoxia-ischemia injury in neonatal mice via a PI3K/Akt-dependent mechanism. *Drug Des Devel Ther*. 2021;15:517–529. doi: 10.2147/DDDT.S293025
35. Guo Z, Li CS, Wang CM, Xie YJ, Wang AL. CSE/H2S system protects mesenchymal stem cells from hypoxia and serum deprivation-induced apoptosis via mitochondrial injury, endoplasmic reticulum stress and PI3K/Akt activation pathways. *Mol Med Rep*. 2015;12:2128–2134. doi: 10.3892/mmr.2015.3651
36. Lin F, Yang Y, Wei S, Huang X, Peng Z, Ke X, Zeng Z, Song Y. Hydrogen sulfide protects against high glucose-induced human umbilical vein endothelial cell injury through activating PI3K/Akt/eNOS pathway. *Drug Des Devel Ther*. 2020;14:621–633. doi: 10.2147/DDDT.S242521
37. Liu Y, Liao R, Qiang Z, Zhang C. Pro-inflammatory cytokine-driven PI3K/Akt/Sp1 signalling and H2S production facilitates the pathogenesis of severe acute pancreatitis. *Biosci Rep*. 2017;37:BSR20160483. doi: 10.1042/BSR20160483
38. Calvert JW, Elston M, Nicholson CK, Gundewar S, Jha S, Elrod JW, Ramchandran A, Lefer DJ. Genetic and pharmacologic hydrogen sulfide therapy attenuates ischemia-induced heart failure in mice. *Circulation*. 2010;122:11–19. doi: 10.1161/CIRCULATIONAHA.109.920991
39. Huang S, Li H, Ge J. A cardioprotective insight of the cystathionine gamma-lyase/hydrogen sulfide pathway. *Int J Cardiol Heart Vasc*. 2015;7:51–57. doi: 10.1016/j.ijcha.2015.01.010
40. Wen X, Xi Y, Zhang Y, Jiao L, Shi S, Bai S, Sun F, Chang G, Wu R, Hao J, et al. DR1 activation promotes vascular smooth muscle cell apoptosis via up-regulation of CSE/H2 S pathway in diabetic mice. *FASEB J*. 2022;36:e22070. doi: 10.1096/fj.202101455R
41. Terzuoli E, Monti M, Vellecco V, Bucci M, Cirino G, Ziche M, Morbidelli L. Characterization of zofenoprilat as an inducer of functional angiogenesis through increased H2 S availability. *Br J Pharmacol*. 2015;172:2961–2973. doi: 10.1111/bph.13101
42. Wang SS, Chen YH, Chen N, Wang LJ, Chen DX, Weng HL, Dooley S, Ding HG. Hydrogen sulfide promotes autophagy of hepatocellular carcinoma cells through the PI3K/Akt/mTOR signaling pathway. *Cell Death Dis*. 2017;8:e2688. doi: 10.1038/cddis.2017.18
43. Dong C, Chen Z, Zhu L, Bsoul N, Wu H, Jiang J, Chen X, Lai Y, Yu G, Gu Y, et al. Diallyl trisulfide enhances the survival of multiteritory perforator skin flaps. *Front Pharmacol*. 2022;13:809034. doi: 10.3389/fphar.2022.809034
44. Metz HE, Houghton AM. Insulin receptor substrate regulation of phosphoinositide 3-kinase. *Clin Cancer Res*. 2011;17:206–211. doi: 10.1158/1078-0432.CCR-10-0434
45. Cai SL, Tee AR, Short JD, Bergeron JM, Kim J, Shen J, Guo R, Johnson CL, Kiguchi K, Walker CL. Activity of TSC2 is inhibited by AKT-mediated phosphorylation and membrane partitioning. *J Cell Biol*. 2006;173:279–289. doi: 10.1083/jcb.200507119
46. Rossig L, Jadidi AS, Urbich C, Badorff C, Zeiher AM, Dimmeler S. Akt-dependent phosphorylation of p21(Cip1) regulates PCNA binding and proliferation of endothelial cells. *Mol Cell Biol*. 2001;21:5644–5657. doi: 10.1128/MCB.21.16.5644-5657.2001
47. Zhou F, Chang Z, Zhang L, Hong YK, Shen B, Wang B, Zhang F, Lu G, Tvorogov D, Alitalo K, et al. Akt/protein kinase B is required for lymphatic network formation, remodeling, and valve development. *Am J Pathol*. 2010;177:2124–2133. doi: 10.2353/ajpath.2010.091301
48. Choi I, Lee S, Kyoung Chung H, Suk Lee Y, Eui Kim K, Choi D, Park EK, Yang D, Ecoiffier T, Monahan J, et al. 9-cis retinoic acid promotes lymphangiogenesis and enhances lymphatic vessel regeneration: therapeutic implications of 9-cis retinoic acid for secondary lymphedema. *Circulation*. 2012;125:872–882. doi: 10.1161/CIRCULATIONAHA.111.030296
49. Szabo C, Papapetropoulos A. Hydrogen sulphide and angiogenesis: mechanisms and applications. *Br J Pharmacol*. 2011;164:853–865. doi: 10.1111/j.1476-5381.2010.01191.x
50. Saha S, Chakraborty PK, Xiong X, Dwivedi SK, Mustafi SB, Leigh NR, Ramchandran R, Mukherjee P, Bhattacharya R. Cystathionine beta-synthase regulates endothelial function via protein S-sulfhydration. *FASEB J*. 2016;30:441–456. doi: 10.1096/fj.15-278648
51. Weiler MJ, Cribb MT, Nepiyushchikh Z, Nelson TS, Dixon JB. A novel mouse tail lymphedema model for observing lymphatic pump failure during lymphedema development. *Sci Rep*. 2019;9:10405. doi: 10.1038/s41598-019-46797-2

# Supplemental Material

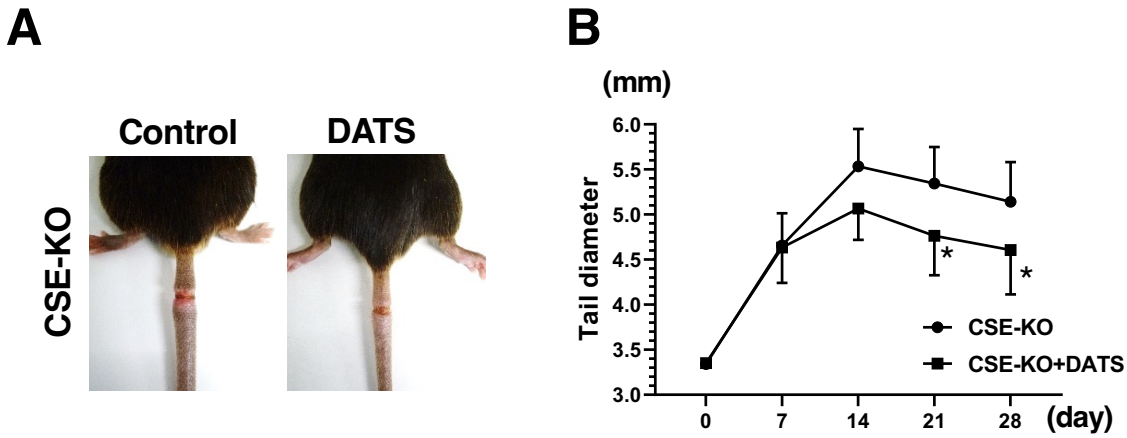


**Figure S1. DATS treatment ameliorates lymphedema in murine tail lymphedema of CSE-KO mice.** (A) Representative pictures of tail lymphedema in CSE-KO mice administered with or without DATS. (B) Changes in the tail diameters after the surgery. Data are mean  $\pm$  SEM ( $n = 8$  for each). \* $P < 0.05$  vs the respective CSE-KO-Control by 2-way ANOVA and Sidak's post hoc tests.

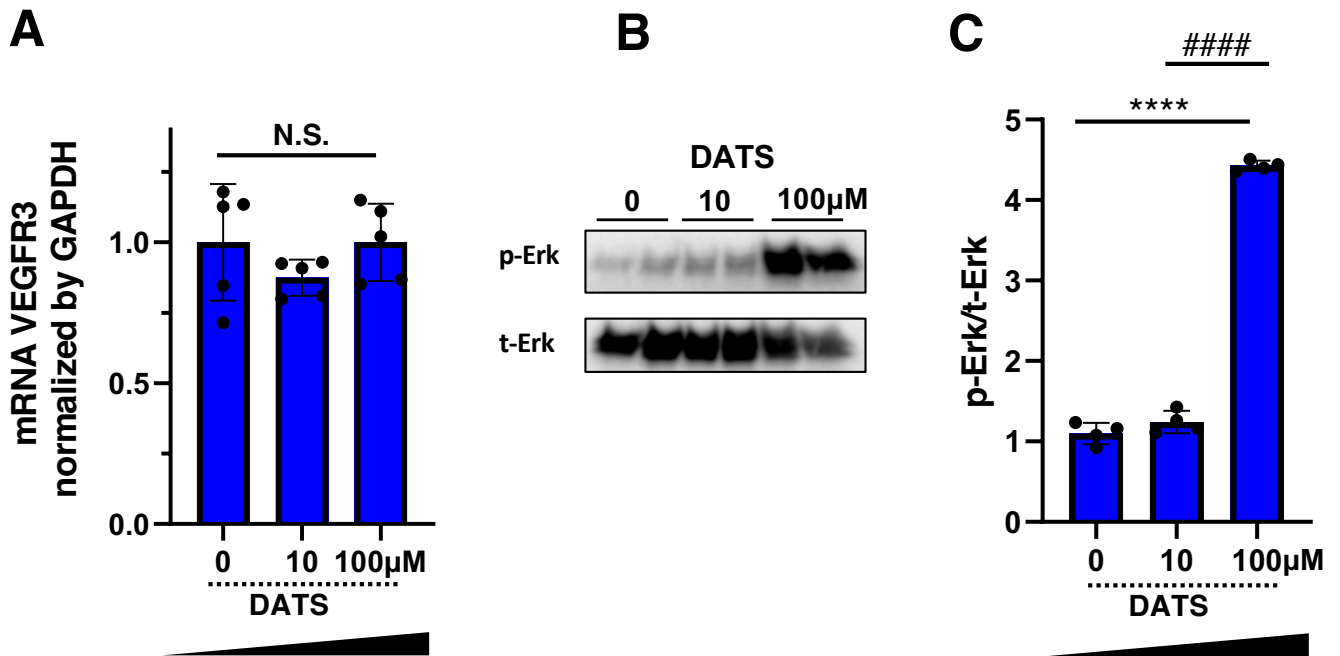


**Figure S2. The reaction of VEGFR3 expression or Erk phosphorylation in LECs after DATS treatment.** (A) The expression of mRNA VEGFR3 in LECs after DATS treatment. Data are mean  $\pm$  SEM ( $n = 5$  each). (B) Representative immunoblots of phospho-Erk and total Erk after DATS treatment. (C) Quantitative analysis of Erk phosphorylation. Data are mean  $\pm$  SEM ( $n = 4$  each). \*\*\*\* $P < 0.0001$  vs 0  $\mu\text{M}$  and ##### $P < 0.0001$  vs 10  $\mu\text{M}$  by 1-way ANOVA and Tukey's *post hoc* tests.



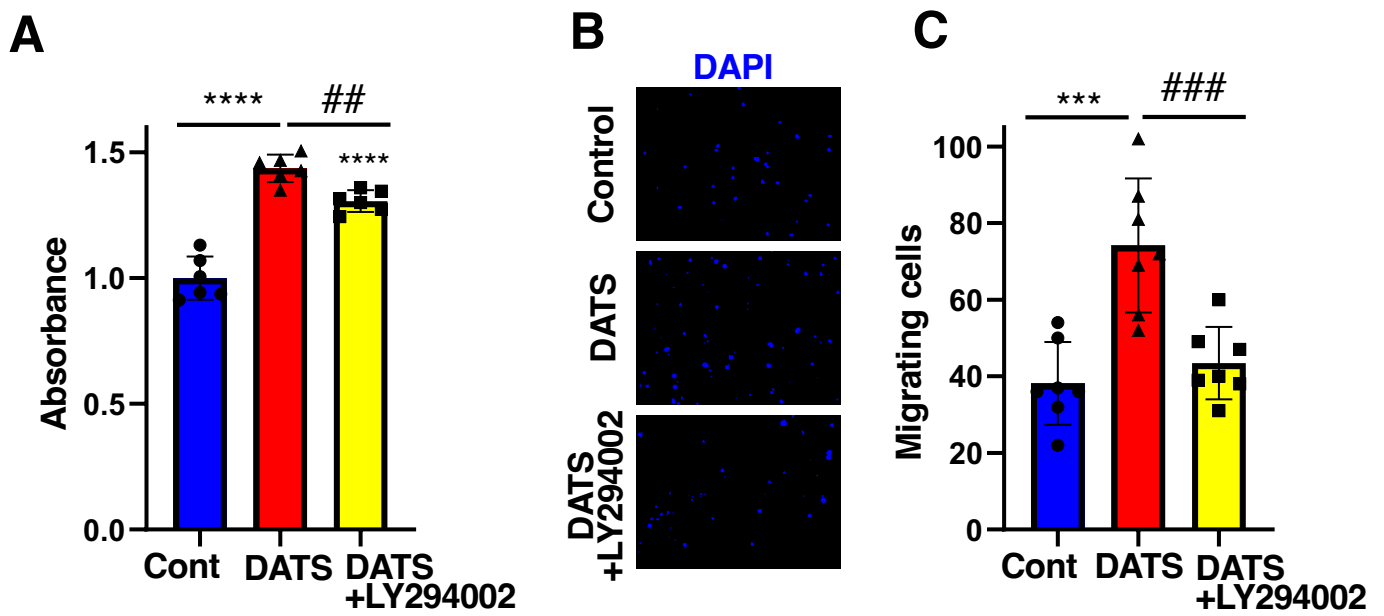


**Figure S3. Inhibition of PI3K/Akt pathway with LY294002 partially impedes DATS-induced lymphangiogenesis *in vitro*** (A) WST-1 proliferation assay of LECs in response to treatments with DATS or DATS + LY294002 ( $n = 6$  for each). \*\*\*\* $P < 0.0001$  vs control and ## $P < 0.01$  vs DATS by 1-way ANOVA and Tukey's *post hoc* tests. (B) Representative images of DAPI-stained migrating cells. (C) Quantitative analysis of migrating cells. Data are mean  $\pm$  SEM ( $n = 7$  for each). \*\*\* $P < 0.001$  vs control and ### $P < 0.001$  vs DATS by 1-way ANOVA and Tukey's *post hoc* tests.